

FewSOL: A Dataset for Few-Shot Object Learning in Robotic Environments

Jishnu Jaykumar P, Yu-Wei Chao, Yu Xiang

Abstract—We introduce the Few-Shot Object Learning (FEWSOL) dataset for object recognition with a few images per object. We captured 336 real-world objects with 9 RGB-D images per object from different views. Object segmentation masks, object poses and object attributes are provided. In addition, synthetic images generated using 330 3D object models are used to augment the dataset. We investigated (i) few-shot object classification and (ii) joint object segmentation and few-shot classification with the state-of-the-art methods for few-shot learning and meta-learning using our dataset. The evaluation results show the presence of a large margin to be improved for few-shot object classification in robotic environments¹.

I. INTRODUCTION

For robots to work in human environments, they will encounter various objects in our daily lives. How can we build models to enable robots to recognize all kinds of objects and eventually manipulate these objects? In the robotics community, model-based object recognition has been the focus, where 3D models of objects are built and used for recognition. For example, the YCB Object and Model Set [1] has significantly benefited 6D object pose estimation and manipulation research. The limitation of model-based object recognition is that it is difficult to obtain a large number of 3D models for many objects in the real world. The 3D scanning techniques are expensive and certain object categories such as reflective objects and transparent objects cannot be reconstructed well. Another paradigm for object recognition focuses on recognizing object categories such as bowls, mugs and bottles. Most datasets for object category recognition only contain few dozen categories. For instance, the MSCOCO dataset for object detection and segmentation [2] has 80 categories. The NOCS dataset for object category pose estimation [3] only has 6 categories. While large-scale datasets collected from the Internet such as ImageNet [4] and Visual Genome [5] contain large numbers of object categories, these datasets are useful for learning visual representations. However, Internet images are not very suitable to learn object representations for robot manipulation due to the domain differences.

In order to overcome the limitations of model-based and category-based approaches for object recognition, in this work, we introduce a new dataset to facilitate object

recognition in robotic environments. We are motivated by few-shot learning and meta-learning in the literature [6]. Our aspiration is that, if robots can recognize objects from a few exemplar images, it is possible to scale up the number of objects a robot can recognize, since collecting a few images per object is a much easier process compared to building a 3D model of an object. In addition, models trained in the meta-learning setting [7] can generalize to new objects without re-training.

In our Few-Shot Object Learning (FEWSOL) dataset, we have collected images for 336 objects in the real world. For each object, we collected 9 RGB-D images from different views, i.e., 9 shots per object. We provide ground truth segmentation masks and 6D object poses of these objects, where the object poses are computed using AR tags. In addition, we employed Amazon Mechanical Turk (MTurk) to collect annotations of these objects including object names, object categories, materials, function and colors. For each object, we collected annotations from 5 MTurkers and then merged their answers. In this way, we can account for how different people name these objects in our dataset. Based on the collected object names, we have defined 198 classes for these 336 objects. In few-shot learning or meta-learning settings, we can think of these images as support sets. Our goal is to apply learned models to cluttered scenes. Therefore, we include the images from the Object Clutter Indoor Dataset (OCID) [8] in our dataset. Segmentation masks of objects are provided in the OCID dataset. We manually annotated class names of these objects, and found that they belong to 52 classes in our object categories. These images can be used as query sets.

To further expand the scale of our dataset, we also generate synthetic data to complement the data from the real world. We selected 330 3D object models from the Google Scanned Objects dataset [19] and used the PyBullet simulator to compose synthetic scenes of these objects and render synthetic RGB-D images from the scenes. Similar to the real-world data, we first put each 3D model onto a table and generate 9 views. The benefit of using synthetic data is that we can generate cluttered scenes with these objects and obtain annotations for all the objects. We generate 40,000 cluttered scenes and render 7 views per scene.

In this paper, we use our dataset to study two problems: (i) few-shot object classification and (ii) joint object segmentation and few-shot classification. For few-shot classification, we follow the protocol proposed in the Meta-Dataset [20] which constructs episodes for training and testing. Each episode consists of multiple support sets and query sets with

Jishnu Jaykumar P and Yu Xiang are with the Department of Computer Science, University of Texas at Dallas, Richardson, TX 75080, USA {jishnu.p, yu.xiang}@utdallas.edu

Yu-Wei Chao is with NVIDIA, Seattle, WA 98105, USA ychao@nvidia.com

¹Dataset and code available at

<https://irvlutd.github.io/FewSOL>

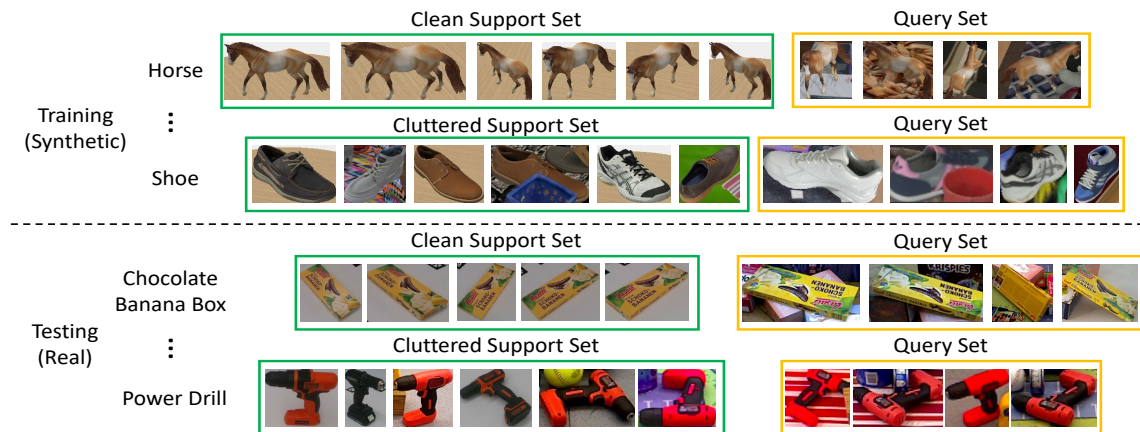


Fig. 1: Examples of support sets and query sets from our dataset. Clean support sets only contain images with single objects in clean background, while cluttered support sets have images with multiple objects and different background.

Dataset	Class type	#classes	Image Type	#images_per_class	Annotations
Omniglot [9]	Characters	1623	RGB	20	class label
mini-ImageNet [10]	WordNet synsets	100	RGB	600	class label
ILSVRC-2012 [11]	WordNet synsets	1000	RGB	≈8,004	class label
Aircraft [12]	Aircraft	100	RGB	100	class label
CUB-200-2011 [13]	Birds	200	RGB	≈59	class label
Describable Texture [14]	Textures	47	RGB	120	class label
Quick Draw [15]	Drawings	345	RGB	≈146,164	class label
Fungi [16]	Fungal species	1394	RGB	≈65	class label
VGG Flower [17]	Flowers	102	RGB	≈81	class label
Traffic Signs [18]	Traffic signs	43	RGB	≈912	class label
MSCOCO [2]	Internet Objects	80	RGB	≈10,751	class label, segmentation
Ours (real + synthetic)	Daily objects	198 + 125	RGB-D	≈27 + 10,234	class label, segmentation, object pose and attribute

TABLE I: Comparison of our dataset with other datasets for few-shot learning in the literature.

different number of classes and images per class. Fig. 1 illustrates some support sets and query sets from our dataset. We reserve the cluttered images from the OCID dataset for testing, and limit training to synthetic data only. In this way, we can investigate sim-to-real transfer for few-shot learning with our dataset. We use the ground truth segmentation masks to crop the objects for classification. For joint object segmentation and few-shot classification, we first apply an object segmentation method and then use the predicted masks to crop the objects for classification. Therefore, segmentation errors can be accounted for in the classification accuracy. We have evaluated state-of-the-art methods for few-shot learning and meta-learning on these two settings using our dataset. These results can be used for future comparison. To the best of our knowledge, our dataset is the first large-scale dataset for few-shot object learning. Enabling robots to recognize these object categories in our dataset can provide information of objects to downstream tasks such as manipulation, object retrieval or human-robot interaction using object names.

II. RELATED WORK

Few-Shot Learning and Meta-Learning. In the context of image classification, few-shot learning indicates using a few images per class. The problem is usually formulated as “ N -way, k -shot”, i.e., N classes with k images per class. The end goal of few-shot learning is to learn a model on a set of training classes \mathcal{C}_{train} that can generalize to novel classes \mathcal{C}_{test} in testing. Each class has a support set and a query set. While the ground truth labels of both the support

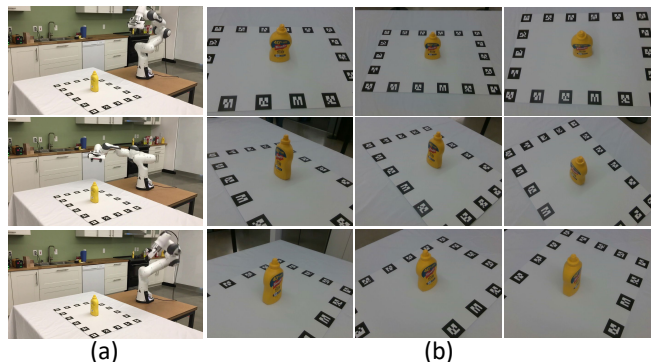


Fig. 2: (a) Our data capture system with a Franka Emika Panda arm. (b) 9 images of a mustard bottle from different views captured.

set and the query set for a class in \mathcal{C}_{train} are available for learning, for a testing class in \mathcal{C}_{test} , only labels of the support set are available. Non-episodic approaches using all the data in \mathcal{C}_{train} for training such as k -NN and its ‘Finetuned’ variants [21], [22], [23], [24]. These methods focus on learning feature representations using neural networks that can be used in \mathcal{C}_{test} . Episodic approaches are considered to be meta-learners. An episode in training or testing consists of a subset of classes with support and query sets. Learning is performed by minimizing the loss on the query sets of the training episode. Representative episodic approaches include Prototypical Networks [25], Matching Networks [10], Relation Networks [26], Model Agnostic Meta-Learning (MAML) [7], Proto-MAML [20] and CrossTransformers [27]. We evaluated majority of these

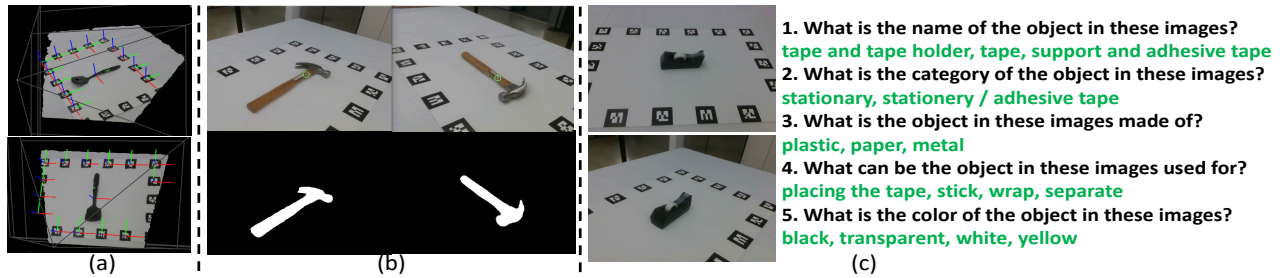


Fig. 3: (a) Object poses from AR tags (b) Pixel correspondences using computed object poses and the segmentation masks of the objects. (c) Our Amazon Mechanical Turk questionnaire for object annotation.

state-of-the-art few-shot learning methods on FEWSOL.

Datasets for Few-Shot Learning. The Omniglot [9] and the mini-ImageNet [10] are widely used for evaluating few-shot learning methods in the literature. Recently, the Meta-Dataset [20] was introduced for benchmarking few-shot learning and meta-learning methods. Meta-Dataset leverages data from 10 different datasets: ILSVRC-2012 (ImageNet [11]), Omniglot [9], Aircraft [12], CUB-200-2011 (Birds [13]), Describable Textures [14], Quick Draw [15], Fungi [16], VGG Flower [17], Traffic Signs [18] and MSCOCO [2]. As we can see, these data do not include daily objects for robot manipulation. Our dataset complements existing datasets for few-shot learning by explicitly addressing robotic applications. Table I compares our FewSOL dataset with existing datasets for few-shot learning. We provide both real and synthetic RGB-D images and more annotations for objects. It is worth mentioning that the CO3D [28] dataset for 3D reconstruction has the potential to be used for few-shot object learning.

III. DATASET CONSTRUCTION

A. Data Capture in the Real World

For each object in the real world, we capture multiple exemplar images of the object. We automate this process using a Franka Emika Panda arm as shown in Fig. 2(a). An Intel RealSense D415 camera is mounted onto the Panda arm gripper. It can capture both RGB images and depth images. We specify 9 waypoints of the camera pose and utilize motion planning of the arm to move the camera to these poses. For each object, we can automatically capture 9 RGB-D images from 9 different views (Fig. 2(b), 3 poses on the left, 3 poses in the front and 3 poses on the right).

In order to accurately estimate the camera poses of these 9 images with respect to the object, we have designed a marker board with 18 AR tags. During data capture, we place the object in the center of the board. For each captured image, we use the detected AR tag poses in the image to compute the camera pose with respect to the center of the marker board and treat this pose as the estimated object pose of the image. Because there are noises in the AR tag poses, we use the RANSAC algorithm to estimate the object pose in this process. Fig. 3(a) shows the AR tag poses and the computed object poses with the point clouds from the RealSense camera. Using the object poses and the point clouds, we can also compute pixel correspondences between images as shown in Fig. 3(b). Consequently, we obtain 9

RGB-D images with their estimated object poses for each object. We have captured 336 objects in total. These include various daily objects from grocery stores and tools.

B. Data Annotation

After capturing these objects, our next step is to provide annotations for these objects. First, we generate the segmentation masks of these captured objects. Instead of manually segmenting these objects, we utilize the unseen object instance segmentation method proposed in [29]. The trained network in [29] cannot successfully segment all the objects in the beginning. Therefore, we bootstrap the network by finetuning it on our dataset. After applying the network on all the data, we manually select accurate segmentation for finetuning, and then apply the finetuned network to unsuccessful images. We iterate this process until all the objects can be segmented by the network. Fig. 3(b) shows two examples of the generated segmentation masks.

Second, we provide object class labels and additional attributes for these objects. We leverage Amazon Mechanical Turk (MTurk) for this annotation. In this way, we can gather how lay people name the classes and attributes of the objects, which can be useful to deploy object recognition systems to real-world robotic scenarios. We designed 5 questions for each object and ask MTurkers to answer these questions. For each object, we gather answers from 5 different MTurkers and merge their answers. Fig. 3(c) illustrates an example with the questions and the merged answers. These annotations can be used to recognize detailed attributes of objects. Based on these annotations from MTurk, we define 198 object classes for these 336 captured objects. Since 9 images are captured for each object, on average, each class has around 15 images in our dataset.

C. Synthetic Data Generation

Leveraging synthetic data for learning has been successful in various robotic problems such as object segmentation [29], grasping [30] and control policy learning [31], since one can generate large-scale synthetic data with ground truth annotations automatically. In our dataset, we also leverage synthetic images for few-shot object learning. To do so, we selected 330 3D object models from Google Scanned Objects [19]. We use these 3D models to generate two types of data. First, similar to our real-world data capture, we place each object onto a table in the PyBullet simulator and generate 9 RGB-D images of each object from 9 different

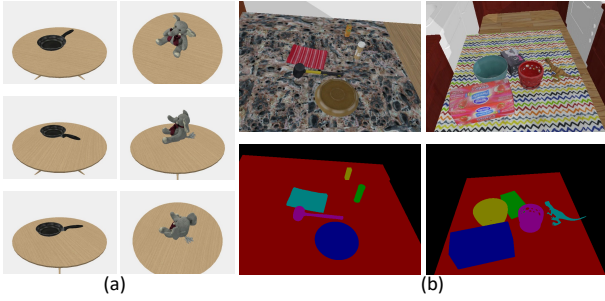


Fig. 4: (a) Synthetic objects with clean background. (b) Synthetic objects in cluttered scenes.

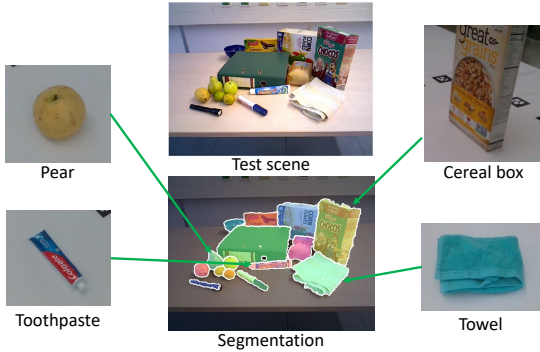


Fig. 5: Illustration of the joint object segmentation and few-shot classification problem with an image from the OCID dataset [8].

views. Fig 4(a) shows some examples of these multi-view images. Second, we generate cluttered scenes using these objects as shown in Fig 4(b). Thanks to the simulator, we can obtain object segmentation masks of these images effortlessly, which is otherwise time-consuming to collect from cluttered scene in the real world. We generated 40,000 scenes of these objects on tabletops and rendered 7 RGB-D images per scene. In order to obtain class names of these 330 objects, we also employ MTurk to collect annotations of these objects as described in Sec. III-B. Eventually, we define 125 classes for these synthetic objects.

D. Joint Object Segmentation and Few-Shot Classification

In real-world robotic applications, objects usually appear in cluttered scenes. Therefore, we need to separate an object from other objects plus the background and then classify it. For our dataset, we target at the problem of joint object segmentation and few-shot classification. The problem is illustrated in Fig. 5. Given an image of a cluttered scene, the task is to segment objects in the scene and classify each object in few-shot learning settings. In order to evaluate the performance on joint object segmentation and few-shot classification on real-world images, we leverage the Object Clutter Indoor Dataset (OCID) proposed in [8]. This dataset was originally proposed for object segmentation. It provides segmentation masks of objects in the dataset. We manually annotate objects in the OCID dataset with class labels. We found that there are 2300 objects in the OCID dataset after filtering a few bad segmentation annotations. These objects belong to 52 classes in our dataset. Objects in OCID can be partially occluded which makes the few-shot object classification challenging.

E. Training and Testing

Our goal in building this dataset is to develop perception models that can classify objects in cluttered scenes with few examples per class. Therefore, we reserve the objects in the OCID dataset for testing, which are real-world objects in cluttered scenes (Fig. 5). For training, we use the synthetic images rendered using Google Scanned Objects. The reasons for using synthetic data for training are: i) it is easy to generate cluttered scenes with ground truth annotations; ii) we can study sim-to-real transfer with our dataset.

In few-shot learning or meta-learning settings, both training and testing have a support set and a query set. During training, the labels of the support set and the query set are available. So we can use the labels on the query set to compute the training loss. During testing, labels of the support set are provided and the goal is to infer labels of the query set. Testing classes can be different from the training classes. When using our dataset, we consider two types of support sets: *clean support sets* and *cluttered support sets*. Clean support sets only consist of images of clean background without occlusions, while cluttered support sets contain images with different background and occlusions. Fig. 1 illustrates these two types of support sets and their query sets. Since query images are from cluttered scenes, training with clean support sets is more challenging. However, if a method can work well with clean support sets, it requires less annotations, i.e., no annotation from cluttered scenes is needed. For example, given a novel object, we can just collect a few images of the object in a clean background in order to recognize it. Therefore, we encourage models that can perform well with clean support sets in our dataset.

IV. BENCHMARKING EXPERIMENTS

In this section, we evaluate the state-of-the-art methods for few-shot learning and meta-learning on our dataset.

A. Few-Shot Object Classification

First, we follow the training and testing procedure designed in Meta-Dataset [20] and evaluated the following methods on our dataset: k -NN baseline that classifies each query example to the class of its closest support example, Finetune baseline that trains a classifier on top of the feature embedding using the support set of a test episode, Prototypical Networks [25], Matching Networks [10], first-order Model Agnostic Meta-Learning (fo-MAML) [7], first-order Proto-MAML (fo-Proto-MAML) introduced in [20] and CrossTransformers (CTX) [27]. CTX uses an attention mechanism to compute a ‘query-aligned’ prototype for each class, and then use these prototypes as in Prototypical Networks. [27] also introduces using SimCLR [32] as training episodes by treating every image as its own class for self-supervised learning (CTX+SimCLR). Details about the training and testing setup can be found in the supplementary materials. 95% confidence intervals for the few-shot classification accuracy of these methods are presented in Table II.

Training of these methods is performed on 112 classes of our synthetic dataset, and testing is conducted on 52

Method	OCID (Real) [8]						Google (Synthetic) [19]	
	All (52 classes)		Unseen (41 classes)		Seen (11 classes)		Unseen (13 classes)	
	Cluttered S	Clean S	Cluttered S	Clean S	Cluttered S	Clean S	Cluttered S	Clean S
Training setting: clean support set without pre-training								
<i>k</i> -NN [20]	52.92 ± 1.08	16.19 ± 0.74	55.12 ± 1.08	16.73 ± 0.62	55.90 ± 1.08	31.94 ± 0.89	83.43 ± 0.76	79.91 ± 0.79
Finetune [20]	57.96 ± 1.08	28.99 ± 0.92	62.45 ± 1.13	33.14 ± 0.91	58.49 ± 1.01	36.46 ± 1.04	63.36 ± 1.75	66.60 ± 1.19
ProtoNet [25]	45.02 ± 0.89	16.18 ± 0.74	50.00 ± 0.91	17.20 ± 0.72	48.90 ± 0.88	32.73 ± 0.89	71.62 ± 0.98	72.63 ± 0.79
MatchingNet [10]	51.58 ± 1.08	19.40 ± 0.72	58.24 ± 1.04	21.70 ± 0.76	53.99 ± 1.02	33.10 ± 0.94	76.26 ± 0.82	77.26 ± 0.76
fo-MAML [7]	24.24 ± 1.17	17.01 ± 1.00	30.29 ± 1.33	19.09 ± 0.86	41.82 ± 0.95	41.82 ± 0.95	51.31 ± 1.70	59.54 ± 0.96
fo-Proto-MAML [20]	49.57 ± 1.00	20.06 ± 0.79	55.96 ± 1.04	22.51 ± 0.73	55.32 ± 1.03	33.45 ± 0.95	68.70 ± 1.42	81.69 ± 0.80
CTX [27]	53.17 ± 1.05	18.49 ± 0.84	55.81 ± 0.99	20.60 ± 0.94	56.77 ± 0.98	35.41 ± 0.93	86.46 ± 0.70	88.08 ± 0.63
CTX+SimCLR [27]	53.87 ± 1.03	30.31 ± 1.00	56.56 ± 0.97	30.43 ± 0.93	64.90 ± 0.98	53.70 ± 1.18	85.15 ± 0.69	83.94 ± 0.65
Training setting: cluttered support set without pre-training								
<i>k</i> -NN [20]	58.78 ± 1.04	21.72 ± 0.84	61.56 ± 1.13	22.17 ± 0.78	66.33 ± 1.02	41.76 ± 1.00	86.94 ± 0.67	80.99 ± 0.69
Finetune [20]	58.63 ± 1.12	29.94 ± 0.90	63.18 ± 1.06	32.71 ± 0.89	59.28 ± 1.07	39.71 ± 1.01	66.36 ± 1.77	65.02 ± 1.24
ProtoNet [25]	42.56 ± 0.88	15.17 ± 0.82	47.60 ± 0.87	16.23 ± 0.77	48.93 ± 0.89	33.69 ± 1.02	71.21 ± 0.97	66.76 ± 0.87
MatchingNet [10]	52.94 ± 1.09	17.98 ± 0.77	56.20 ± 1.05	19.52 ± 0.73	54.07 ± 1.03	31.18 ± 0.93	78.51 ± 0.82	72.25 ± 0.87
fo-MAML [7]	43.92 ± 1.07	17.26 ± 0.87	49.21 ± 1.03	18.80 ± 0.80	51.94 ± 1.00	28.91 ± 0.92	70.78 ± 0.90	66.54 ± 0.88
fo-Proto-MAML [20]	51.00 ± 1.02	17.35 ± 0.75	55.46 ± 1.06	19.59 ± 0.74	56.90 ± 1.06	31.99 ± 0.91	76.78 ± 1.10	77.36 ± 0.83
CTX [27]	49.96 ± 1.04	18.43 ± 0.74	53.91 ± 1.02	20.82 ± 0.87	57.97 ± 0.98	36.93 ± 1.03	92.45 ± 0.46	89.82 ± 0.58
CTX+SimCLR [27]	60.83 ± 1.06	31.67 ± 0.97	63.80 ± 1.09	33.34 ± 0.99	66.25 ± 1.01	51.62 ± 1.10	89.58 ± 0.57	88.99 ± 0.57
Training setting: clean support set with pre-training								
<i>k</i> -NN [20]	59.34 ± 1.10	23.40 ± 0.85	63.02 ± 1.07	24.98 ± 0.86	66.24 ± 1.01	39.36 ± 1.01	89.18 ± 0.59	85.77 ± 0.69
Finetune [20]	59.77 ± 1.08	32.15 ± 0.90	64.01 ± 1.08	35.54 ± 0.90	58.30 ± 1.09	37.72 ± 1.04	66.09 ± 1.72	69.85 ± 1.09
ProtoNet [25]	57.54 ± 1.06	34.47 ± 1.00	61.25 ± 1.11	37.06 ± 1.01	65.90 ± 1.04	51.07 ± 1.04	74.37 ± 1.12	81.38 ± 0.67
MatchingNet [10]	53.81 ± 1.02	26.33 ± 0.94	57.77 ± 0.93	28.05 ± 1.00	61.83 ± 0.97	45.81 ± 1.07	65.40 ± 1.57	85.18 ± 0.70
fo-MAML [7]	44.92 ± 1.20	15.71 ± 0.77	51.67 ± 1.13	17.74 ± 0.77	56.02 ± 1.04	30.78 ± 0.95	70.91 ± 1.08	73.86 ± 0.88
fo-Proto-MAML [20]	57.09 ± 1.04	27.01 ± 0.94	60.29 ± 1.02	28.69 ± 0.88	66.75 ± 1.04	44.39 ± 1.10	77.16 ± 1.10	88.14 ± 0.68
CTX [27]	56.65 ± 1.02	29.06 ± 0.99	60.33 ± 1.02	29.96 ± 0.94	65.47 ± 1.04	45.48 ± 1.12	90.66 ± 0.63	92.72 ± 0.45
CTX+SimCLR [27]	57.47 ± 1.03	31.29 ± 0.98	59.32 ± 0.98	31.31 ± 0.93	67.73 ± 0.91	53.67 ± 1.14	81.76 ± 0.74	82.76 ± 0.74
Training setting: cluttered support set with pre-training								
<i>k</i> -NN [20]	60.63 ± 1.10	23.09 ± 0.87	62.54 ± 1.12	23.97 ± 0.77	65.16 ± 1.04	40.82 ± 1.04	89.21 ± 0.55	84.49 ± 0.74
Finetune [20]	60.11 ± 1.12	31.23 ± 0.95	62.58 ± 1.10	33.22 ± 0.94	58.89 ± 1.03	36.48 ± 1.06	66.49 ± 1.73	68.31 ± 1.15
ProtoNet [25]	59.02 ± 1.00	31.86 ± 1.02	61.56 ± 1.09	34.12 ± 1.06	66.47 ± 0.94	48.80 ± 1.12	79.49 ± 0.94	79.19 ± 0.78
MatchingNet [10]	62.35 ± 1.06	28.50 ± 0.93	65.41 ± 1.06	30.16 ± 0.94	70.50 ± 0.99	44.01 ± 1.03	85.44 ± 0.63	84.10 ± 0.70
fo-MAML [7]	56.04 ± 1.08	20.64 ± 0.76	58.01 ± 1.12	21.24 ± 0.81	58.81 ± 1.12	32.38 ± 0.96	79.12 ± 0.95	71.88 ± 1.00
fo-Proto-MAML [20]	60.98 ± 1.01	28.32 ± 0.91	63.18 ± 1.02	29.08 ± 0.93	71.44 ± 1.00	46.98 ± 1.07	89.21 ± 0.70	86.70 ± 0.71
CTX [27]	56.29 ± 0.93	26.93 ± 0.91	58.52 ± 0.92	27.40 ± 0.95	63.00 ± 1.01	44.11 ± 1.06	94.51 ± 0.39	92.06 ± 0.48
CTX+SimCLR [27]	62.70 ± 1.07	38.56 ± 1.12	64.86 ± 1.09	38.22 ± 1.07	73.11 ± 0.93	61.47 ± 1.11	89.23 ± 0.60	90.01 ± 0.49

TABLE II: Benchmarking results on few-shot object classification in terms of 95% confidence intervals for classification accuracy with *episodic testing* consisting of 600 episodes as in Meta-Dataset [20].

classes in the OCID dataset [8] and 13 validation classes in the synthetic dataset. The backbones of these methods are ResNet-34 except for the Finetune baseline (ResNet-18 due to GPU memory limit). As in Meta-Dataset [20], we compare with and without pre-training for the backbone network, where pre-training initializes the backbone weights as the *k*-NN Baseline model trained on ImageNet. We also use either clean support sets or cluttered support sets during training. The choice of pre-training and support set generates four training settings as shown in Table II. For testing episodes, we evaluate on both clean support sets and cluttered support sets as well.

For the results in Table II, we have the following observations. i) Adding pre-training is beneficial. Most classification accuracies are improved with pre-training. ii) The performance on the synthetic classes is much better than the performance on the real classes. We can see the sim-to-real gap clearly. iii) Using cluttered support sets can achieve better performance than using clean support sets. Because query sets contain different background and occlusions. However, obtaining annotations for cluttered support sets in the real world is expensive. Methods using clean support sets in testing are encouraged. iv) Among the 52 classes in OCID, we separately tested on 41 unseen classes, i.e., novel classes not presented in training, and 11 seen classes. Overall, the performance on seen classes is better. v) Among these evaluated methods, CrossTransformers [27] achieves the best performance. When using clean support sets, CTX+SimCLR has a large margin compared to other methods, highlighting the importance of self-supervised representation learning in SimCLR [32]. This experiment suggests that pre-training

and self-supervised contrastive representation learning can be critical in few-shot learning and meta-learning.

B. Joint Object Segmentation and Few-Shot Classification

In this experiment, we conduct non-episodic testing on all the 2,300 objects among the 52 classes in the OCID dataset. When cropping objects from the original images for classification, we tested using ground truth masks versus using the predicted masks from [29]. When using predicted masks, we need to assign a mask to each object. This is achieved by the Hungarian method with pairwise F-measure that computes a matching between predicted masks and ground truth objects. These cropped objects construct the query set. We use the real-world objects that we captured on a tabletop as the clean support sets. We present top-1 and top-5 classification accuracies of the evaluated methods in Table III. Few-shot learning methods are trained on the 112 classes of our synthetic dataset with pre-training. In addition, we also tested the CLIP models [33], [34] with different image encoder backbones. If an object cannot be segmented by a segmentation method, i.e., no assigned mask for the Hungarian matching, we consider this object as a misclassification. In this way, the classification accuracy also accounts for the segmentation performance, and using ground truth segmentation masks focuses on evaluating the classification performance only. For Table III, we can see that: i) The top-1 accuracy is around 25% for the best few-shot learning method trained on synthetic data, which indicates that there is still a large margin to be improved in this setting. The difficulties lie in using synthetic images for training and using clean support sets during testing. ii)

Method	OCID (Real) [8]					
	Use GT segmentation (#classes, #objects)			Use segmentation from [29] (#classes, #objects)		
	All (52, 2300)	Unseen (41, 1598)	Seen (11, 702)	All (52, 2300)	Unseen (41, 1598)	Seen (11, 702)
Clean S	Clean S	Clean S	Clean S	Clean S	Clean S	
Training setting: clean support set with pre-training (top-1, top-5)						
k-NN [20]	14.65, 25.22	15.33, 24.41	41.03, 72.65	12.70, 23.22	13.70, 22.59	36.75, 67.95
Finetune [20]	22.26, 50.17	26.41 , 58.20	31.62, 80.34	21.30, 48.57	24.34 , 53.94	35.47, 67.38
ProtoNet [25]	25.17 , 57.30	25.22, 58.45	51.99, 94.73	22.96 , 51.96	22.65, 54.32	49.86, 87.75
MatchingNet [10]	17.39, 48.35	14.64, 50.06	51.85, 90.31	15.78, 45.13	13.08, 46.93	49.15, 84.47
fo-MAML [7]	11.43, 31.48	11.58, 34.73	36.89, 69.94	10.91, 29.17	10.01, 32.35	31.77, 63.68
fo-Proto-MAML [20]	14.35, 28.96	5.63, 40.61	45.58, 71.51	13.39, 26.96	5.51, 37.73	41.74, 67.24
CTX [27]	17.48, 46.57	18.21, 49.81	51.85, 87.75	15.70, 43.83	16.90, 46.31	47.86, 81.34
CTX+SimCLR [27]	18.57, 50.30	20.46, 51.06	57.55 , 93.16	16.48, 46.17	17.71, 47.12	52.14 , 85.75
Training setting: cluttered support set with pre-training (top-1, top-5)						
k-NN [20]	13.70, 23.83	15.33, 24.28	47.72, 72.79	13.26, 23.22	14.14, 22.90	44.73, 68.66
Finetune [20]	22.17, 53.35	24.34, 55.63	31.91, 71.51	18.26, 44.22	20.65, 52.00	36.04, 69.52
ProtoNet [25]	21.35, 50.57	22.34, 51.31	51.99, 90.46	18.61, 47.22	18.21, 48.12	45.44, 85.33
MatchingNet [10]	17.52, 50.96	17.77, 52.32	49.43, 88.18	16.52, 46.52	15.58, 48.81	43.45, 82.76
fo-MAML [7]	16.48, 38.52	13.70, 39.49	37.46, 77.07	15.35, 35.04	11.08, 34.36	40.31, 69.94
fo-Proto-MAML [20]	11.04, 28.70	4.01, 38.67	43.73, 72.65	9.91, 26.35	3.57, 35.79	40.46, 68.09
CTX [27]	19.00, 45.48	17.71, 44.74	51.85, 88.75	17.13, 42.22	16.08, 42.12	47.15, 83.19
CTX+SimCLR [27]	24.61 , 62.39	25.16 , 63.52	65.81 , 96.30	22.17 , 57.43	23.28 , 57.57	59.12 , 88.32
Using pre-trained CLIP models [33]						
Few-shot Tip-Adapter ViT-L/14-Finetune [34]	60.17 , 83.04	59.64 , 85.17	85.75, 99.00	54.87 , 78.91	56.07 , 80.29	79.20, 91.88
Few-shot Tip-Adapter ViT-L/14 [34]	56.78, 83.22	55.38, 84.86	86.89 , 98.58	52.35, 76.26	51.69, 79.04	80.06 , 92.45
Zero-shot CLIP ViT-L/14 [33]	54.57, 84.74	55.94, 87.92	83.62, 98.58	50.43, 78.52	52.07, 81.54	75.07, 92.17
Zero-shot CLIP ViT-B/32 [33]	41.87, 75.26	41.30, 77.91	78.06, 97.58	39.83, 69.43	39.17, 72.09	70.66, 90.88
Zero-shot CLIP ViT-B/16 [33]	40.70, 73.96	40.24, 76.03	76.50, 95.73	39.35, 68.83	38.61, 70.15	70.66, 88.89
Zero-shot CLIP RN50x64 [33]	42.96, 75.83	43.62, 77.41	76.64, 96.01	40.04, 70.87	41.74, 72.22	69.94, 90.46
Zero-shot CLIP RN50x16 [33]	38.52, 73.04	40.11, 75.72	79.49, 96.30	35.65, 67.30	37.30, 69.77	70.94, 89.74
Zero-shot CLIP RN50x4 [33]	35.96, 68.52	34.42, 70.03	73.93, 95.73	34.00, 63.78	32.48, 65.46	67.95, 88.60
Zero-shot CLIP ResNet-101 [33]	32.96, 68.30	32.67, 69.52	77.49, 96.87	31.09, 63.87	31.85, 65.96	69.66, 89.74
Zero-shot CLIP ResNet-50 [33]	25.91, 58.43	29.04, 64.39	61.40, 93.16	24.70, 55.61	28.04, 61.20	57.69, 86.47

TABLE III: Benchmarking results on joint object segmentation and few-shot classification in terms of top-1 and top-5 classification accuracy with *non-episodic testing* on the OCID dataset [8]. For CLIP-based models, different image encoder backbones are tested: ResNet [35], EfficientNet [36] style ResNet (RN50x4, RN50x16, RN50x64) and Vision Transformers (ViT-B/16, ViT-B/32, ViT-L/14) [37].



Fig. 6: Qualitative classification results with top-5 predictions from our real-world testing with the fine-tuned Tip-Adapter model [34].

Classification accuracies of seen classes are much higher than unseen classes. iii) Overall, CTX+SimCLR achieves the better performance when training with cluttered support sets, while Prototypical Network is better when training with clean support sets. iv) The pre-trained CLIP models [33] perform much better than trained few-shot learners on classifying these objects. We think it is due to the large scale real-world data that CLIP models are trained on. The Tip-Adapter [34] adapts CLIP models for few-shot classification. Its training-free model and the fine-tuned variant improve over the original CLIP models.

C. Qualitative Results in the Real World

In this experiment, our goal is to build a few-shot classification model that works the best on real-world perception systems. So we train CTX+SimCLR [27] with all the real data and the synthetic data in our dataset, and then test the trained model in our lab. Cluttered support sets are used for training. RGB-D images are collected from a Fetch mobile manipulator and we used [29] for object segmentation. We tested on 32 objects with 4 objects in an image. The CTX+SimCLR model achieves 28.13% and 56.25%, the pre-trained CLIP-ViT-L/14 model achieves 65.63% and

81.25% and the fine-tuned Tip-Adapter (ViT-L/14) model achieves 65.63% and 84.38% top-1 and top-5 accuracy, respectively. Fig. 6 shows one testing image and the classification results from the Tip-Adapter [34] model. Please see the supplementary video for these classification results. The low top-1 accuracy indicates the difficulty of the few-shot object classification problem in the real world. Most failure cases in few-shot classification are due to the differences between testing objects and training objects. How to achieve better generalization in few-shot object classification is an interesting direction to explore in the future. We hope that our dataset can be used to build better models for this problem.

V. CONCLUSION AND FUTURE WORK

We introduce the Few-Shot Object Learning (FEWSOL) dataset for few-shot object recognition. Different from existing datasets for few-shot learning, our dataset contains household objects such as personal items, tools and fruits. We provide RGB-D images, object segmentation masks, object poses and object attribute annotations in the dataset. We hope the dataset can facilitate progress on robot object perception. If a robot can recognize all the object classes in the dataset (198 classes of real objects), this will help lots of robotic applications such as manipulation, object retrieval, object grounding, task planning, and so on. We demonstrated using our dataset for (i) few-shot object classification and (ii) joint object segmentation and few-shot classification in this paper. From the experimental results, we see a need to improve the few-shot recognition performance for real-world robotic applications. In the future, we plan to study how to leverage depth data and multi-view information to improve few-shot object classification. We also plan to study few-shot object representation learning for shape reconstruction, object pose estimation and object attribute recognition using the FEWSOL dataset.

ACKNOWLEDGMENTS

This work was supported in part by the DARPA Perceptually-enabled Task Guidance (PTG) Program under contract number HR00112220005.

REFERENCES

- [1] B. Calli, A. Walsman, A. Singh, S. Srinivasa, P. Abbeel, and A. M. Dollar, "Benchmarking in manipulation research: The YCB object and model set and benchmarking protocols," *arXiv preprint arXiv:1502.03143*, 2015.
- [2] T.-Y. Lin, M. Maire, S. Belongie, J. Hays, P. Perona, D. Ramanan, P. Dollár, and C. L. Zitnick, "Microsoft COCO: Common objects in context," in *European Conference on Computer Vision (ECCV)*. Springer, 2014, pp. 740–755.
- [3] H. Wang, S. Sridhar, J. Huang, J. Valentin, S. Song, and L. J. Guibas, "Normalized object coordinate space for category-level 6D object pose and size estimation," in *IEEE/CVF Conference on Computer Vision and Pattern Recognition (CVPR)*, 2019, pp. 2642–2651.
- [4] J. Deng, W. Dong, R. Socher, L.-J. Li, K. Li, and L. Fei-Fei, "ImageNet: A large-scale hierarchical image database," in *IEEE Conference on Computer Vision and Pattern Recognition (CVPR)*. Ieee, 2009, pp. 248–255.
- [5] R. Krishna, Y. Zhu, O. Groth, J. Johnson, K. Hata, J. Kravitz, S. Chen, Y. Kalantidis, L.-J. Li *et al.*, "Visual genome: Connecting language and vision using crowdsourced dense image annotations," *International Journal of Computer Vision (IJCV)*, vol. 123, no. 1, pp. 32–73, 2017.
- [6] Y. Wang, Q. Yao, J. T. Kwok, and L. M. Ni, "Generalizing from a few examples: A survey on few-shot learning," *ACM computing surveys (CSUR)*, vol. 53, no. 3, pp. 1–34, 2020.
- [7] C. Finn, P. Abbeel, and S. Levine, "Model-agnostic meta-learning for fast adaptation of deep networks," in *International Conference on Machine Learning (ICML)*. PMLR, 2017, pp. 1126–1135.
- [8] M. Suchi, T. Patten, D. Fischinger, and M. Vincze, "Easylabel: A semi-automatic pixel-wise object annotation tool for creating robotic rgb-d datasets," in *International Conference on Robotics and Automation (ICRA)*. IEEE, 2019, pp. 6678–6684.
- [9] B. M. Lake, R. Salakhutdinov, and J. B. Tenenbaum, "Human-level concept learning through probabilistic program induction," *Science*, vol. 350, no. 6266, pp. 1332–1338, 2015.
- [10] O. Vinyals, C. Blundell, T. Lillicrap, D. Wierstra *et al.*, "Matching networks for one shot learning," *Advances in Neural Information Processing Systems (NeurIPS)*, vol. 29, 2016.
- [11] O. Russakovsky, J. Deng, H. Su, J. Krause, S. Satheesh, S. Ma, Z. Huang, A. Karpathy, A. Khosla, M. Bernstein *et al.*, "Imagenet large scale visual recognition challenge," *International Journal of Computer Vision (IJCV)*, vol. 115, no. 3, pp. 211–252, 2015.
- [12] S. Maji, E. Rahtu, J. Kannala, M. Blaschko, and A. Vedaldi, "Fine-grained visual classification of aircraft," *arXiv preprint arXiv:1306.5151*, 2013.
- [13] C. Wah, S. Branson, P. Welinder, P. Perona, and S. Belongie, "The caltech-ucsd birds-200-2011 dataset," 2011.
- [14] M. Cimpoi, S. Maji, I. Kokkinos, S. Mohamed, and A. Vedaldi, "Describing textures in the wild," in *Proceedings of the IEEE Conference on Computer Vision and Pattern Recognition (CVPR)*, 2014, pp. 3606–3613.
- [15] J. Jongejan, H. Rowley, T. Kawashima, J. Kim, , and N. Fox-Gieg, "The quick, draw! – a.i. experiment, quickdraw.withgoogle.com," 2016.
- [16] M. Sulc, L. Picek, J. Matas, T. Jeppesen, and J. Heilmann-Clausen, "Fungi recognition: A practical use case," in *Proceedings of the IEEE/CVF Winter Conference on Applications of Computer Vision (WACV)*, 2020, pp. 2316–2324.
- [17] M.-E. Nilsback and A. Zisserman, "Automated flower classification over a large number of classes," in *2008 Sixth Indian Conference on Computer Vision, Graphics & Image Processing*. IEEE, 2008, pp. 722–729.
- [18] S. Houben, J. Stallkamp, J. Salmen, M. Schlipsing, and C. Igel, "Detection of traffic signs in real-world images: The german traffic sign detection benchmark," in *The International Joint Conference on Neural Networks (IJCNN)*. IEEE, 2013, pp. 1–8.
- [19] L. Downs, A. Francis, N. Koenig, B. Kinman, R. Hickman, K. Reymann, T. B. McHugh, and V. Vanhoucke, "Google scanned objects: A high-quality dataset of 3D scanned household items," *arXiv preprint arXiv:2204.11918*, 2022.
- [20] E. Triantafyllou, T. Zhu, V. Dumoulin, P. Lamblin, U. Evci, K. Xu, R. Goroshin, C. Gelada, K. Swersky, P.-A. Manzagol *et al.*, "Meta-dataset: A dataset of datasets for learning to learn from few examples," *arXiv preprint arXiv:1903.03096*, 2019.
- [21] S. Gidaris and N. Komodakis, "Dynamic few-shot visual learning without forgetting," in *Proceedings of the IEEE Conference on Computer Vision and Pattern Recognition (CVPR)*, 2018, pp. 4367–4375.
- [22] H. Qi, M. Brown, and D. G. Lowe, "Low-shot learning with imprinted weights," in *Proceedings of the IEEE Conference on Computer Vision and Pattern Recognition (CVPR)*, 2018, pp. 5822–5830.
- [23] W.-Y. Chen, Y.-C. Liu, Z. Kira, Y.-C. F. Wang, and J.-B. Huang, "A closer look at few-shot classification," *arXiv preprint arXiv:1904.04232*, 2019.
- [24] Y. Tian, Y. Wang, D. Krishnan, J. B. Tenenbaum, and P. Isola, "Rethinking few-shot image classification: a good embedding is all you need?" in *European Conference on Computer Vision (ECCV)*. Springer, 2020, pp. 266–282.
- [25] J. Snell, K. Swersky, and R. Zemel, "Prototypical networks for few-shot learning," *Advances in Neural Information Processing Systems (NeurIPS)*, vol. 30, 2017.
- [26] F. Sung, Y. Yang, L. Zhang, T. Xiang, P. H. Torr, and T. M. Hospedales, "Learning to compare: Relation network for few-shot learning," in *Proceedings of the IEEE Conference on Computer Vision and Pattern Recognition (CVPR)*, 2018, pp. 1199–1208.
- [27] C. Doersch, A. Gupta, and A. Zisserman, "Crosstransformers: spatially-aware few-shot transfer," *Advances in Neural Information Processing Systems (NeurIPS)*, vol. 33, pp. 21 981–21 993, 2020.
- [28] J. Reizenstein, R. Shapovalov, P. Henzler, L. Sbordone, P. Labatut, and D. Novotny, "Common objects in 3d: Large-scale learning and evaluation of real-life 3d category reconstruction," in *Proceedings of the IEEE/CVF International Conference on Computer Vision*, 2021, pp. 10 901–10 911.
- [29] Y. Xiang, C. Xie, A. Mousavian, and D. Fox, "Learning RGB-D feature embeddings for unseen object instance segmentation," in *Conference on Robot Learning (CoRL)*. PMLR, 2021, pp. 461–470.
- [30] J. Mahler, J. Liang, S. Niyaz, M. Laskey, R. Doan, X. Liu, J. A. Ojea, and K. Goldberg, "Dex-net 2.0: Deep learning to plan robust grasps with synthetic point clouds and analytic grasp metrics," *arXiv preprint arXiv:1703.09312*, 2017.
- [31] Y. Chebotar, A. Handa, V. Makoviychuk, M. Macklin, J. Issac, N. Ratliff, and D. Fox, "Closing the sim-to-real loop: Adapting simulation randomization with real world experience," in *International Conference on Robotics and Automation (ICRA)*. IEEE, 2019, pp. 8973–8979.
- [32] T. Chen, S. Kornblith, M. Norouzi, and G. Hinton, "A simple framework for contrastive learning of visual representations," in *International Conference on Machine Learning (ICML)*. PMLR, 2020, pp. 1597–1607.
- [33] A. Radford, J. W. Kim, C. Hallacy, A. Ramesh, G. Goh, S. Agarwal, G. Sastry, A. Askell, P. Mishkin, J. Clark *et al.*, "Learning transferable visual models from natural language supervision," in *International Conference on Machine Learning*. PMLR, 2021, pp. 8748–8763.
- [34] R. Zhang, Z. Wei, R. Fang, P. Gao, K. Li, J. Dai, Y. Qiao, and H. Li, "Tip-adapter: Training-free adaption of clip for few-shot classification," *arXiv preprint arXiv:2207.09519*, 2022.
- [35] K. He, X. Zhang, S. Ren, and J. Sun, "Deep residual learning for image recognition," in *Proceedings of the IEEE conference on computer vision and pattern recognition*, 2016, pp. 770–778.
- [36] M. Tan and Q. Le, "Efficientnet: Rethinking model scaling for convolutional neural networks," in *International conference on machine learning*. PMLR, 2019, pp. 6105–6114.
- [37] A. Kolesnikov, A. Dosovitskiy, D. Weissenborn, G. Heigold, J. Uszkoreit, L. Beyer, M. Minderer, M. Dehghani, N. Houlsby, S. Gelly, T. Unterthiner, and X. Zhai, "An image is worth 16x16 words: Transformers for image recognition at scale," 2021.